Journal of Chromatography A, 1534 (2018) 111–122

Contents lists available at ScienceDirect

Journal of Chromatography A

journal homepage: www.elsevier.com/locate/chroma

Comprehensive quantitative analysis of fatty-acyl-Coenzyme A species in biological samples by ultra-high performance liquid chromatography–tandem mass spectrometry harmonizing hydrophilic interaction and reversed phase chromatography

László Abrankó, Gary Williamson, Samantha Gardner, Asimina Kerimi*

University of Leeds, School of Food Science and Nutrition, Leeds, LS2 9JT, UK

ARTICLE INFO

Article history:
Received 8 August 2017
Received in revised form
18 December 2017
Accepted 19 December 2017
Available online 23 December 2017

Keywords:
Acyl-CoA
UHPLC–ESI-MS/MS
Phosphorylated organic molecules
Liver
Cells
Lipid biomarkers

ABSTRACT

Fatty acyl-Coenzyme A species (acyl-CoAs) are key biomarkers in studies focusing on cellular energy metabolism. Existing analytical approaches are unable to simultaneously detect the full range of short-, medium-, and long-chain acyl-CoAs, while chromatographic limitations encountered in the analysis of limited amounts of biological samples are an often overlooked problem. We report the systematic development of a UHPLC–ESI-MS/MS method which incorporates reversed phase (RP) and hydrophilic interaction liquid chromatography (HILIC) separations in series, in an automated mode. The protocol outlined encompasses quantification of acyl-CoAs of varying hydrophobicity from C2 to C20 with recoveries in the range of 90–111 % and limit of detection (LOD) 1–5 fmol, which is substantially lower than previously published methods. We demonstrate that the poor chromatographic performance and signal losses in MS detection, typically observed for phosphorylated organic molecules, can be avoided by the incorporation of a 0.1% phosphoric acid wash step between injections. The methodological approach presented here permits a highly reliable, sensitive and precise analysis of small amounts of tissues and cell samples as demonstrated in mouse liver, human hepatic (HepG2) and skeletal muscle (LHCNM2) cells. The considerable improvements discussed pave the way for acyl-CoAs to be incorporated in routine targeted lipid biomarker profile studies.

1. Introduction

Fatty acids originating from the diet or *de novo* synthesized are intracellularly processed in their activated form following esterification with Coenzyme A. Fatty acyl-CoAs are key effectors at the crossroads of converging metabolic pathways [1] and thought to act as signaling intermediates in insulin resistance and related diseases [1,2]. Despite extensive research on the role of acyl-CoAs in mitochondrial dysfunction and the metabolic syndrome, details of direct mechanisms have not yet been identified, highlighting the need for more robust analytical methods to enable comprehensive profiling of acyl-CoAs in different matrices and models. While liquid chromatography followed by electrospray ionization tandem mass spectrometric detection (LC–ESI-MS/MS) has been routinely employed, most methods are capable of only detecting either short-, medium-, or long-chain acyl-CoAs [3–8]. Although their MS detection is well characterized, chromatography remains the most challenging part of the technique due to the structural complexity of the compounds. Even with advances in the latest generation of LC–MS systems and their superior analytical power *per se*, problems encountered with small amounts of biological samples requiring enhanced sensitivity have not been adequately addressed. The majority of published protocols rely on the well-established selected reaction monitoring (SRM) or multiple reaction monitoring (MRM) scan mode and monitor the transition that yields the most abundant fragment of acyl-CoAs formed by the cleavage of the 3′-phosphate-adenosine-5′diphosphate subunit of the CoA part of the molecule (Fig. S1) [3,5,7,9–15]. Neutral loss [9,16,17] and precursor ion scanning [11,18] have also been utilized, enabling a non-targeted profiling approach. In comparison, reported chromatographic approaches vary considerably implying that an optimal method has not been established yet. To adapt for ESI-MS detection, phosphate buffer used in earlier protocols employing LC separation by UV at slightly

* Corresponding author.
E-mail address: a.kerimi@leeds.ac.uk (A. Kerimi).

https://doi.org/10.1016/j.chroma.2017.12.052

acidic pH (4.5–5.5) is substituted with a volatile buffer(s) such as ammonium-formate [4,12,19] or highly alkaline mobile phase conditions (pH ~10–11) adjusted with NH_4OH solution [7,17]. Methods applying ion pairing chromatography using triethyl amine [10] or dimethylbutyl amine have also been reported [6].

Depending on chain length, acyl-CoAs vary greatly in polarity, and this has become the bottleneck in developing comprehensive methods [4,6,7,18,19]. In addition, severe peak tailing, signal deterioration and poor detection limits are often observed in LC–MS analysis of acyl-CoAs, especially for later eluting species [8,9,16,18–20]. In comparison, the potential of hydrophilic interaction liquid chromatography (HILIC) for the highly polar acyl-CoAs has not been fully explored [21].

We initially conducted experiments to better understand what causes the poor chromatographic behavior of acyl-CoAs. This approach facilitated the development of an improved automated UHPLC-ESI-MS/MS analytical protocol combining both reversed phase (RP) and HILIC separations in series, capable of resolving and quantifying acyl-CoAs in biological tissues ranging from short-chain (e.g. acetyl (C2)) to long-chain (e.g. arachidonoyl (C20)).

2. Experimental section

2.1. Chemicals

Crystalline malonyl-CoA (C3, referred to as malonyl), ($^{13}C_3$)malonyl-CoA, 3-hydroxybutyryl-CoA (3OH-C4), acetyl-CoA (C2), butyryl-CoA (C4), isovaleryl-CoA (*i*C5), *n*-heptanoyl-CoA (C7), *n*-ocanoyl-CoA (C8), lauroyl-CoA (C12), palmitoleoyl-CoA, *cis*-9 (C16:1), palmitoyl-CoA (C16), *n*-heptadecanoyl-CoA (C17), oleoyl-CoA, *cis*-9 (C18:1), stearoyl-CoA (C18), arachidonoyl-CoA (C20), high purity ammonia solution and glacial acetic acid (Trace SELECT), LC–MS grade ammonium bicarbonate, triethylammonium acetate (TEAA) and dexamethasone were purchased from Sigma-Aldrich (Dorset, UK). The *n*-hexanoyl-CoA (C6), *n*-decanoyl-CoA (C10), myristoyl-CoA (C14) and linoleoyl-CoA, *cis*-9, *cis*-12 (C18:2) were from Avanti Polar Lipids (Alabaster, AL, USA) and *n*-pentanoyl-CoA (C5) was from Advent Bio (Downers Grove, IL, USA). Newborn calf serum (Invitrogen 16010159), horse serum (Invitrogen 16050130) and basic fibroblast growth factor (bFGF, Gibco PHG6015) were from Thermo Fisher Scientific and epidermal growth factor (EGF, AF-100-15) was from PeproTech (London, UK). All solvents were of UHPLC–MS grade and water used was of high purity (18.2 MΩ cm^{-1}, Milli-Q, Merck Millipore).

2.2. Liquid chromatography

A Thermo Fisher Scientific Vanquish binary UHPLC (Thermo Scientific, Santa Clara, USA) system was used, with a Waters Acquity BEH C18 (2.1 × 50 mm, 1.7 μm) and a BEH HILIC (2.1 × 50 mm, 1.7 μm) column, in-line with guard columns (VanGuard, 2.1 × 5 mm) of matching stationary phases. During the initial stages of developing the chromatographic separations a UV-DAD detector was connected in line to monitor signals at 260 nm, the optimum wavelength for acyl-CoA species [22]. Columns were thermostatted at 30 °C, and a switching valve was used to divert mobile phase to one column at a time at a flow rate of 0.7 ml/min (Fig. 1). Mobile phase A1 consisted of ammonium bicarbonate (10 mM), adjusted to pH 8.5 with high purity ammonia solution, and acetonitrile (ACN) was used as mobile phase B1. Two solutions were introduced to clean the system between injections. Water/ACN/phosphoric acid 40/60/0.1 (v/v) (pH ≈ 2.5) was used as an 'acidic wash' (B2 channel), and 50/50 ACN/water (channel B3) as a 'neutral wash'. For RP separation, gradient elution started at 95% A1/5% B1 and after 0.2 min hold time, B1 was increased linearly to 45% at 1.0 min, 65% at 3.0 min and to 100% at 3.2 min and kept at 100% B1 until 5.0 min. At 5.01 min, 100% B1 was changed to 100% B2 to initiate the 'acidic wash' to pump B. At 5.1 min, eluent was diverted to waste for the cleaning protocol, bypassing the MS, by use of a diverter valve inserted in the flow path between the LC and the MS. After 3 min of acidic wash, at 8.0 min, the selection valve of pump B was switched to 100% B3 'neutral wash' to remove the acidic mobile phase from the system. Following rinsing for 3 min (11.01 min), 100% B1 was selected to exchange mobile phase to 'B1', and after 3 min initial mobile phase composition settings (95% A1/5% B1) were applied. The system was equilibrated for 3 min (until 17.0 min) before the next injection. Eluent flow was diverted back to the MS at 10.5 min.

The gradient program for the HILIC separation started at 5% A1/95% B1, and B1 was decreased linearly to 70% at 3.0 min, 50% at 3.2 min and kept at 50% until 5.0 min. Eluent was diverted to waste at 5.0 min and mobile phase composition was set to 100% B2 ('acidic wash'). After 3 min (8.0 min total), 100% B3 ('neutral wash') was introduced to remove the acidic solution from the system. Following 3 min rinsing, initial mobile phase composition settings (5% A1/95% B1) were applied and the system was equilibrated for 4 min (until 15.0 min) before the next injection and eluent flow was diverted back to the MS at 14.0 min. The total run time for both the analytical protocols in series and the wash step was 32 min.

2.3. Mass spectrometry

A TSQ Quantiva triple quadrupole MS/MS instrument (Thermo Scientific) equipped with a heated electrospray ion source (HESI) was used in positive ion mode with the following settings: spray voltage: 3500 V, sheath gas: 56 (Arb) ≈ 6.2 L/min, auxiliary gas 18 (Arb) ≈ 11.3 L/min, sweep gas: 2 (Arb) ≈ 2.7 L/min, ion transfer tube temperature: 368 °C, vaporizer temperature: 460 °C. When the eluent flow of the LC was not delivered to the MS, the spray voltage on the HESI needle was set to 0V. Mass spectrometer settings for each acyl-CoA were optimized by using commercially available standards (Table S1).

2.4. Sample preparation

Mouse liver tissue (C57BL/6) was purchased from Seralab (Sera Laboratories International Ltd, West Sussex, UK) and pulverized in a cryogenic tissue homogenizer (Cellcrusher Limited, Ireland). 10–30 mg of frozen powder was weighed in a polypropylene vial and an appropriate volume of ice cold extraction solvent mixture was added according to Minkler et al. [23]. Samples were spiked with 20 μL of 2.5 μM ISTD spiking mix (($^{13}C_3$)malonyl- and C17-CoA in MeOH containing 10 mM TEAA) and kept in a dry ice/ethanol cooling bath until further processing by homogenization (Omni TH, Camlab, UK) and solid phase extraction (SPE) as described below.

Human hepatocellular carcinoma cells, HepG2 (HB-8065, ATCC, LGC Promochem, UK), and LHCNM2 immortalized human skeletal muscle cells (a gift from Dr V. Mouly, UMR S 787, INSERM & UPMC, Institut de Myologie, Paris, France) were grown at 37 °C in humidified air with 5% CO_2 as per standard protocols. LHCNM2 cells were grown on 0.2% gelatin-coated tissue culture dishes and differentiation was induced at ~95% confluence by replacing growth medium (Dulbecco's minimum essential modified medium, DMEM, 10% heat-inactivated fetal calf serum, 10% newborn calf serum, EGF, bFGF, dexamethasone) with differentiation medium (DMEM, 2% horse serum) for a period of 5 days before cell harvesting. For analysis, cells were washed twice and collected in ~0.2 mL phosphate buffered saline (PBS) containing phosphatase and protease inhibitors (Roche Diagnostics, Sigma, UK). Cell suspensions were transferred to tubes containing 0.4 mL acetonitrile: isopropanol (3:1 v/v), and extracted for 30 s with a cell disruptor (Disruptor

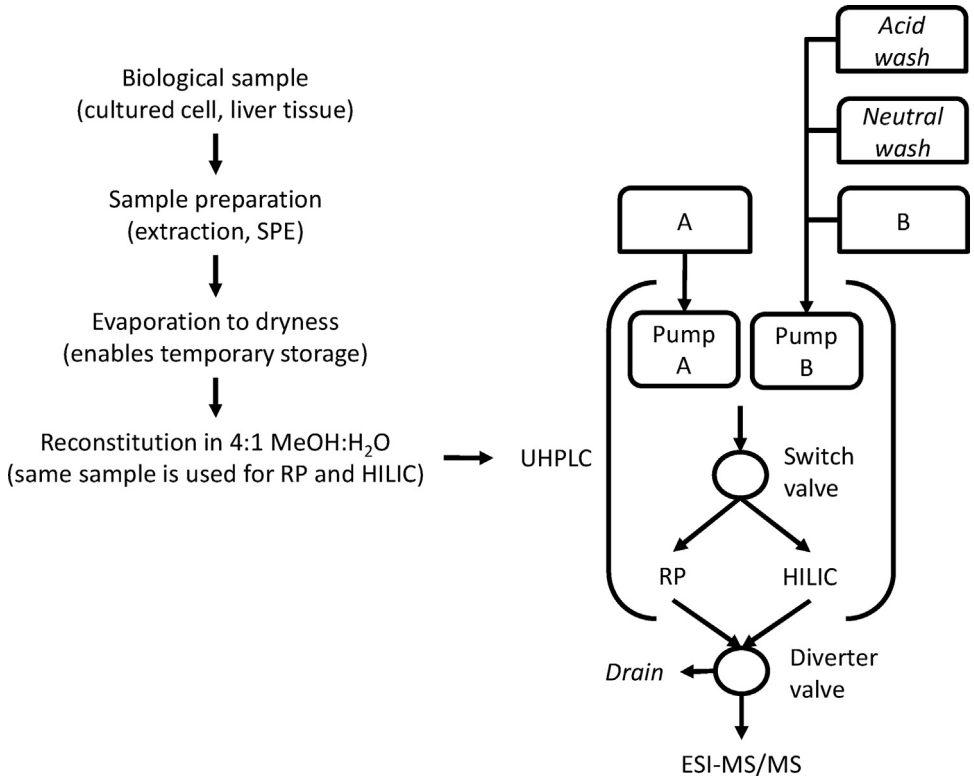

Fig. 1. Overview of the applied setup of the LC–MS system using the dual chromatographic system and the workflow of the harmonized sample preparation protocol.

Genie, Scientific Industries, NY, USA). 100 μL 0.1M phosphate buffer (pH 6.7) and 20 μL of 0.5 μM ISTD spiking mix (C5- and C17-CoA in 10 mM TEAA in MeOH) were added and the samples were further extracted for 30 s. Following centrifugation (5 min, 16,000 x *g*, 4 °C) the supernatant was acidified with 150 μL glacial acetic acid. The cell pellet was retained for protein determination by the BCA protein assay (Pierce, Rockford, IL, USA) following re-solubilization in 2 M urea and 0.5% (m/v) SDS in 50 mM Tris-HCl, (pH 8.0) according to Hummon et al. [24].

Isolation of acyl-CoAs from the supernatant was carried out by SPE with 2-(2-pyridyl)ethyl- functionalized silica sorbent (Sigma-Aldrich, UK) as previously described [23]. The eluate was evaporated to dryness under vacuum at ambient temperature (~2.5 h) in a Genevac EZ2 system (Genevac, SP Scientific, UK) and samples were stored at −80 °C until analysis.

Dried samples were first reconstituted in 10 μL water (20 μL for liver tissues) and full recovery of the dried matter was facilitated with sonication and vortexing. 40 μL MeOH (80 μL for liver tissues) was added and the sonication/vortexing steps were repeated. Samples were centrifuged (21,000 × *g*, 4 °C, 5 min) and 2 μL of the supernatant was injected to the analytical column of the LC–MS.

3. Results and discussion

3.1. Optimization of mass spectrometric settings

Targeted MS analysis of acyl-CoAs employed SRM of the parent compounds and subsequent fragment(s) as defined by infusing original standard solutions to the MS prepared in 10 mM TEAA in MeOH. Although acyl-CoAs are most likely present in their anionic forms in aqueous methanolic solution [25], higher sensitivity was observed in positive ion mode. $[M+H]^+$ was the most abundant parent ion detected, resulting from the loss of NH_3 from $[M+NH_4]^+$ ions in solution, during transition to the gas phase at the final stages of electrospray ionization [26].

Fragmentation of acyl-CoAs in positive ion mode also gives rise to several abundant fragments common to all acyl-CoA species such as *m/z* 136.1, 229.2, 261.1, and 428.0 (Fig. S1). The most dominant fragment results from the cleavage of the 3′-phosphate-adenosine-5′-diphosphate moiety of the molecule and is specific and distinctive for each acyl-CoA as it contains the species-defining fatty-acyl residue (indicated by R in Fig. S1). This fragment was selected as the primary transition while the common fragments at *m/z* 428, *m/z* 261 and *m/z* 136, were used as confirmatory SRM transitions for all monitored acyl-CoAs (Table S1).

3.2. Chromatographic improvements for enhanced sensitivity at low concentrations

RP separation on a C18 column is the preferred method of choice for the analysis of the majority of acyl-CoAs while HILIC separation was essential for the very polar compounds. Overlaid SRM traces of 15 acyl-CoA species obtained with our finalized RP method are shown in Fig. 2A. SRM chromatograms of five selected acyl-CoA standards acquired with the finalized HILIC gradient program are shown in Fig. 2B. The few published chromatographic methods that have attempted to combine analysis of very polar and very long-chain acyl-CoAs without the use of ion-pairing reagents in the mobile phase [12,19] report poor chromatographic behavior and poor sensitivity, especially in the case of the later eluting compounds. Although it is generally accepted that ion-pairing agents such as trimethylamine (TEA) [5,10,14], tributylamine [18], and dimethylbutylamine [6] can enhance the retention and separation of hydrophilic charged/ionizable species on RP columns, such alkylammonium cations can cause significant ion suppression in the ESI source, and were therefore avoided.

However, the addition of TEAA when using pure standards contributed to enhanced stability of the acyl-CoAs in solution and led to better signals. We hypothesize that TEAA is possibly acting as a chelator and blocking silanophilic interactions with the phosphate

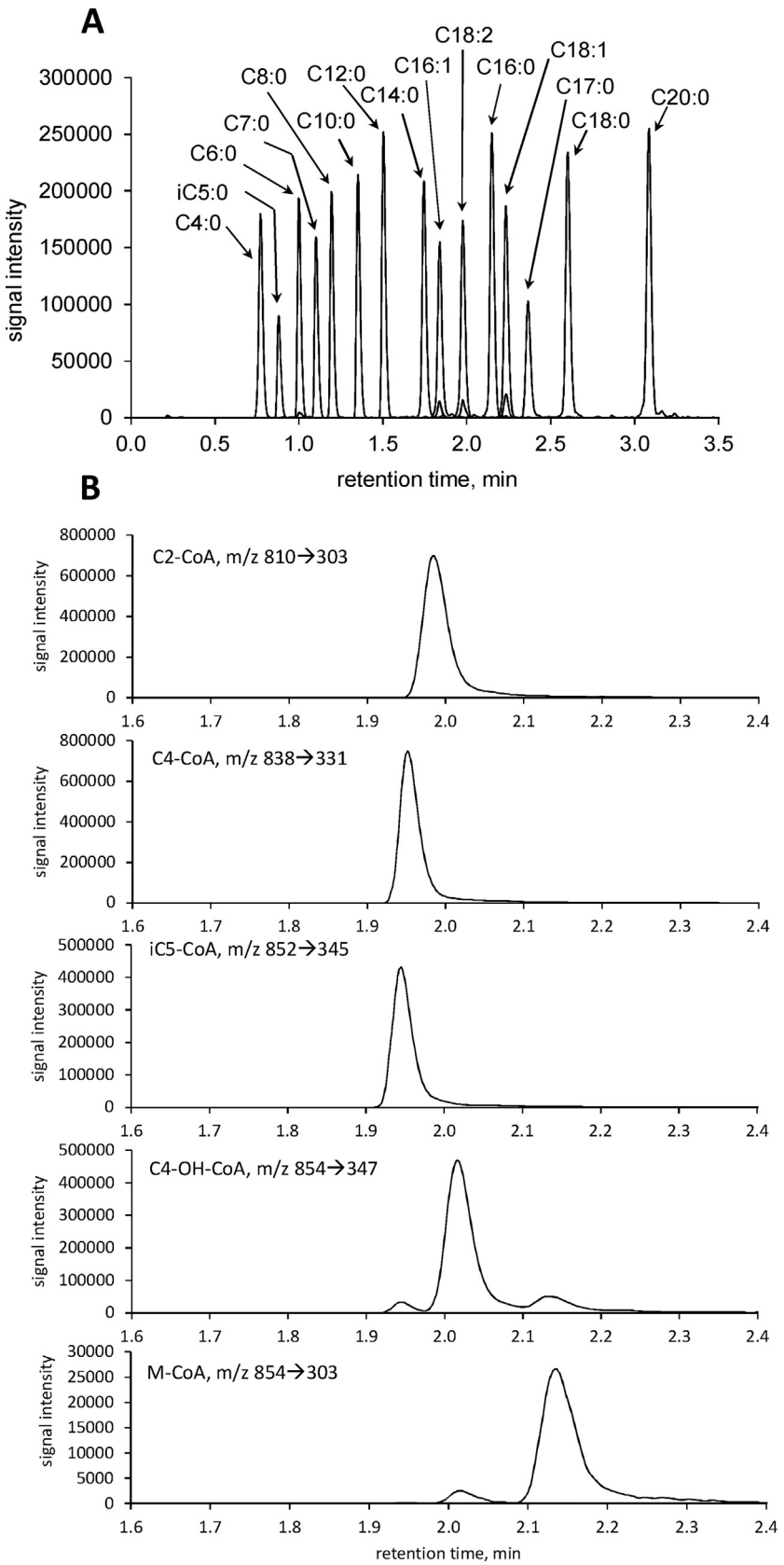

Fig. 2. (A) Overlaid SRM traces of 15 acyl-CoA species in a standard mixture analyzed with reversed phase UHPLC separation. Butyryl-CoA (C4:0), hexanoyl-CoA (C6:0), octanoyl-CoA (C8:0), decanoyl-CoA (C10:0), lauroyl-CoA (C12:0), myristoyl-CoA (C14:0), palmitoleoyl-CoA (C16:1, n-9), palmitoyl-CoA (C16:0), linoleoyl-CoA (C18:2, n-6, n-9), oleoyl-CoA (C18:1, n-9), stearoyl-CoA (C18:0), arachidonoyl-CoA (C20:0) were all at 0.25 μM (500 fmol on column); isovaleryl-CoA (*i*C5) and heptadecanoyl-CoA (C17:0) (both at 0.5 μM, 1 pmol on column) are internal standards. (B) HILIC separation of a standard mixture of acyl-CoA species. SRM traces of acetyl-CoA (C2), butyryl-CoA (C4:0), isovaleryl-CoA (*i*C5), 3-hydroxy-butyryl-CoA (3OH-C4:0) and malonyl-CoA (C3). All at 0.25 μM, 500 fmol on column except for *i*C5 (0.5 μM, 1 pmol on column).

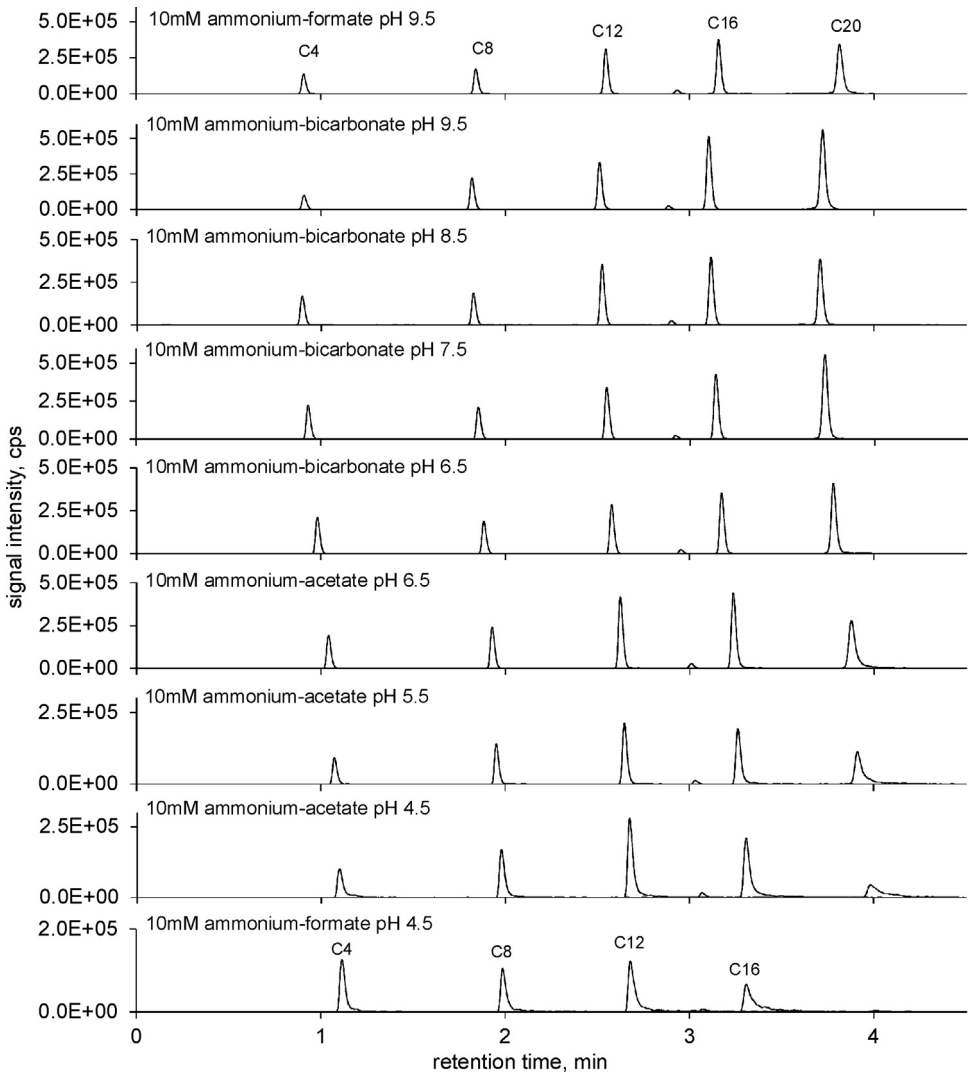

Fig. 3. Effect of the pH and buffer composition of the mobile phase on separation of four representative acyl-CoA species. The primary SRM transitions of butyryl-CoA (C4), octanoyl-CoA (C8), lauroyl-CoA (C12), palmitoyl-CoA (C16) and arachidonoyl-CoA (C20) are shown injected from a mixed standard of 500 fmol each (0.25 μM). Note that arachidonoyl-CoA (C20) was not detected when 10 mM ammonium-formate buffer at pH 4.5 was used as mobile phase A. ACN was used as the organic mobile phase B throughout the experiment.

groups of the acyl-CoAs on the surface of the C18 RP stationary phase as previously reported by others for EDTA and phosphoric acid in the case of peptide analysis [27,28]. Residual unreacted silanol groups are impossible to avoid even with the newest generation of highly end-capped, hybrid, silica-bonded stationary phases such as the one we used for the applications described here, and although less prominent in higher pH they can still interfere with the analysis of compounds bearing multiple charged moieties such as acyl-CoAs.

Guided by the literature [12,15,29,30], we tested RP separations of five representative acyl-CoAs (C4, C8, C12, C16, C20) employing ammonium formate, ammonium acetate and ammonium bicarbonate buffers at varying pH (4.5–9.5, Table S2), with a generic gradient (from 5 to 100% acetonitrile in 5 min). Obtained SRM traces are shown in Fig. 3. In particular, 10 mM ammonium formate or ammonium acetate at pH 4.5 and acetonitrile resulted in strikingly poor chromatographic performance. Analysis of later eluting acyl-CoAs was not possible in both chromatographic systems at 0.25 μM (500 fmol on column of each acyl-CoA, Fig. 3). When a larger injection volume was used for the lower concentration of acyl-CoAs standard mix (e.g. 15 μL of a 5 μM solution), detected peak areas were comparable to those obtained with a 1.5 μL injection of a 50 μM solution. This indicated that analyte loss is not strictly concentration-dependent while signal deterioration was remarkably lower when standard solutions of acyl-CoAs were introduced to the MS by flow injection.

Tuytten et al. [31] previously argued that the primary cause of losses when analyzing phosphorylated organic molecules by LC–ESI-MS is binding of the analytes to the iron (hydr)oxides present on the surface of the stainless steel ESI probe. To explore this possibility, we tested the same protocol for only the UHPLC using UV detection at 260 nm. Standard UV RP traces acquired with ammonium-bicarbonate at pH 9.5 were compared to those acquired with ammonium-formate at pH 4.5 from injections of 0.25, 1.25 and 2.5 μM of a mixture of 14 acyl-CoAs (Fig. 4). The later eluting components suffered a progressive decline in peak height and increase in peak width relative to the early eluting species, while the peak quality deteriorated with replicate injections for acyl chains of >12 carbons. Such analyte loss and peak deterioration was less pronounced at higher concentrations (>50 μM) both in RP and HILIC. The fact that signal losses were already evident by UV detection indicated to us that the stainless steel ESI probe is not the primary cause. However, as pH is a critical factor in such sorption events and given that the process becomes kinetically slow

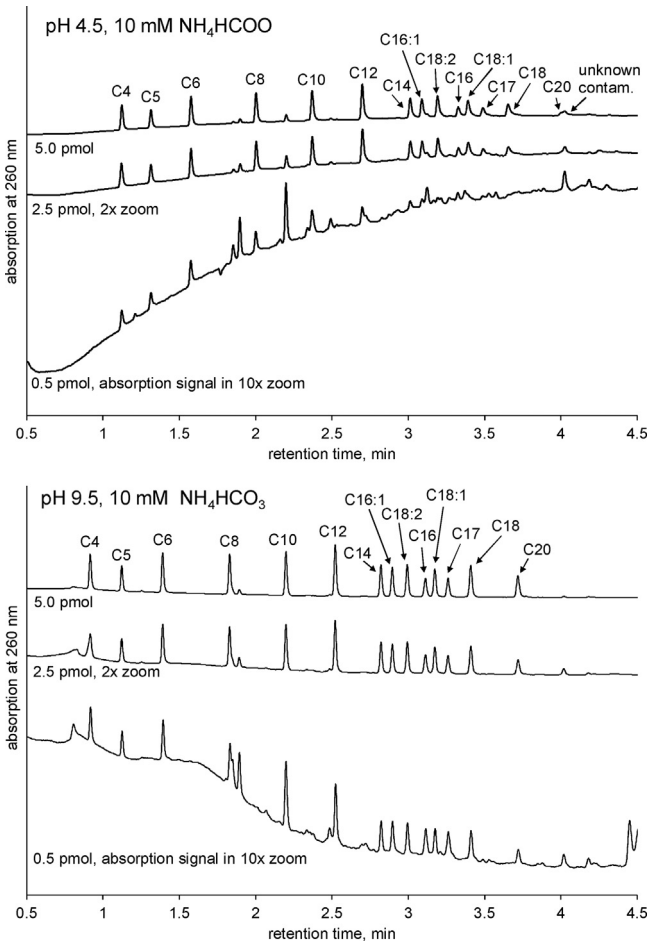

Fig. 4. UHPLC-UV chromatograms of standard mixtures of 14 acyl-CoAs acquired with the same gradient program and different buffer systems as mobile phase A. Ammonium-formate at pH 4.5 is shown in the top panel and ammonium-bicarbonate at pH 9.5 in the bottom panel. Chromatograms of lower concentrations are magnified 2- and 10-fold for 2.5 (1.25 μM) and 5 pmol (2.5 μM) respectively.

only at pH > 8.5 [31], we cannot rule out that the interactions with the ESI stainless steel probe may have a minor contribution to the poor signals observed with ammonium formate and ammonium acetate at pH 4–6.

These lines of evidence led us to the conclusion that the limiting factor in the LC–MS analysis of acyl-CoAs in terms of analytical power at the lower concentration range is the chromatography component rather than the MS part. Typical UHPLC column dimensions (e.g. 50 × 2.1 mm) limit injection volumes to the range of 1–10 μL compared to 10–50 μL volumes possible on standard HPLC columns; this translates to a 10-fold difference in the absolute amount of analyte loaded to the column. To exclude the column specific aspect of acyl-CoA signal losses, we tested the hypothesis that a modest amount of acyl-CoAs is retained on the chromatographic column by comparing RP separation on various columns (Waters X-Bridge 2.1 × 100 mm, 3.5 μm, Phenomenex Kinetex C18 and C8 both 100 Å, 2.1 × 100 mm, 2.6 μm, Shiseido Capcell Pak C18, 2.0 × 100 mm, 3 μm). Comparable signal deterioration was observed in all tested columns.

As an alternative possible cause of the losses, we postulated interactions between divalent cationic (metal) ions, present on the surface of the LC flow path, with the anionic phosphate groups of acyl-CoAs. Metal cations have previously been reported on the stainless steel tubing, the column stainless steel tube and the column frits [32]. Haddad and Foley reported that metal frits accounted for approximately 96% of the total metal surface in contact with eluent therefore being the main source of metal ions and particularly Fe(III) [33]. For example, the interaction of Mg^{2+} with phosphate groups has been previously reported while Mg^{2+} quite effectively precipitates palmitoyl-CoA from solution [34]. Such interactions are also possible under acidic conditions as the 3′-phosphate of the CoA moiety of acyl-CoAs is anionic even at very low pH [25]. In agreement, we observed that signal intensity and peak shape deterioration was more pronounced for later eluting acyl-CoA species at acidic pH where chelation would be more pronounced. Although the hypothesis of metal ions-related precipitation in chromatographic systems is supported by the findings of others [28,32,35], we could not fully explain why the longer chain acyl-CoAs seem to be more affected than the shorter chain ones. Given that signal intensity was influenced by the buffer type and pH (Fig. 3), a logical explanation could be that the shorter chain species suffer smaller losses as they elute at a higher proportion of buffer which is thought to be superior in suppressing metal chelation [36]. In another study of nucleotide analysis by LC–MS, clearly sharper peaks were observed when ammonium bicarbonate was used as the mobile phase, indicating a superior effect on counteracting processes involved in analyte loss [37].

A strong acidic wash with 0.1% phosphoric acid solution in 60% ACN and 40% water introduced in between every injection successfully addressed the issue. At the end of the gradient program, pump B (channel B2) was filled with 60/40/0.1 (v/v) ACN/water/phosphoric acid ('acidic wash'), and ∼10 column volumes were delivered. Avoidance of signal deterioration was achieved, even in the targeted sub μM concentration range. A second wash step to remove the phosphoric acid was necessary. A 'neutral wash' with ∼10 column volumes of 1:1 ACN/water on channel B3 was introduced before equilibration to the starting mobile phase conditions. This automated cleaning protocol successfully prevented peak deterioration, when tested with a 0.5 nM standard mixture solution (1 fmol of each analyte on column).

The critical role of the phosphate ions in the reconditioning step is also supported by the observations of Constantinides and Steim [34] who reported that the solubility of 50 μM palmitoyl-CoA in 50 mM phosphate buffer was little affected by addition of 1–3 mM Mg^{2+} whereas it was completely precipitated when in Tris-HCl buffer. This can also explain the absence of this particular problem in the classic, but much less sensitive, HPLC-UV methods using phosphate buffer as aqueous mobile phase [36], whereas chromatographic problems such as peak tailing, peak distortion [8] as well as sensitivity loss [18] for later eluting compounds (e.g., palmitoyl-CoA, oleoyl-CoA) are much more pronounced in the "LC–MS compatible" mobile phases. Similar observations have been reported for nucleotides [31,37]. When multiple injections were carried out omitting the acidic wash step in between, less analyte loss was observed after several injections with ammonium bicarbonate at pH 9.5 (Fig. 5).

Based on this evidence, we concluded that the use of ammonium-bicarbonate buffer at slightly alkaline pH (pH ≥ 8.5) along with the use of an acidic wash step with 0.1% phosphoric acid solution between injections can efficiently eliminate the observed analyte loss, even at low concentrations. Our data cannot dissect to what extent the phosphoric acid wash simply suppresses interactions with the metal ions on the flow path of the LC or protonates unreacted silanol groups. Whatever the case, we believe it is sufficient to remove retained acyl-CoAs as shown in Fig. 5. In this experiment, we show traces from injections performed in the absence of the acidic wash, followed by a blank injection, a gradient with an acidic wash and afterwards repeat of the same sequence of injections. The later acyl-CoAs retained on the column elute at the expected retention times with progressively increasing peak areas, suggesting to us that they were adsorbed at the head of the column and consecutive injections were not able to elute them. A

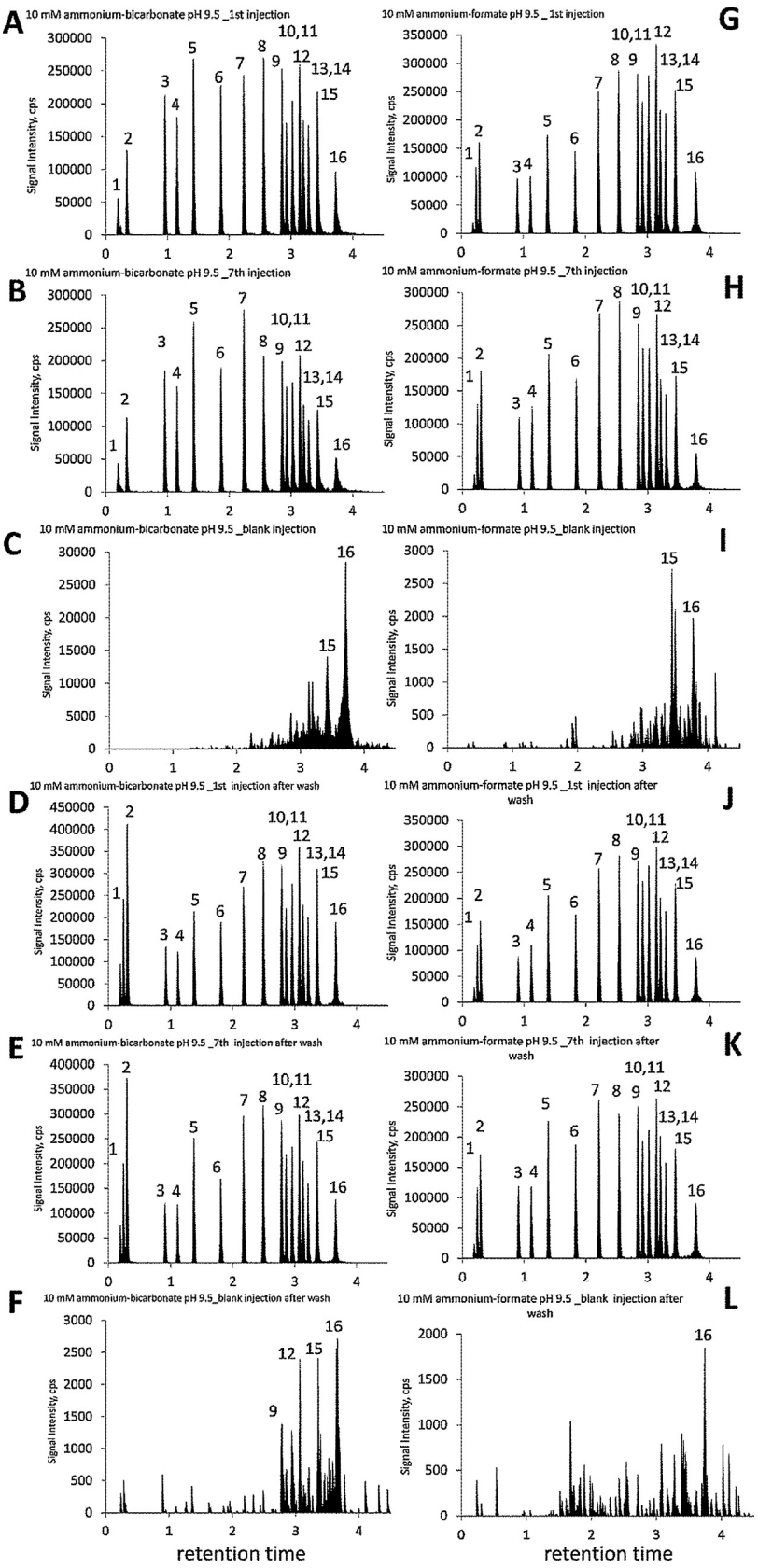

Fig. 5. Signal enhancement of acyl-CoAs following an "acidic wash". The elution profile of 16 acyl-CoAs was compared in ammonium-bicarbonate (pH 9.5, A–F) and ammonium-formate buffer (pH 9.5, G–L) after 1 (A, G) and 7 injections (B, H) in the absence of the acidic wash, followed by a blank injection (C, I). After a single blank injection with a gradient including the acidic wash the same sequence of injections was repeated, 1st (D, J) and 7th (E, K) followed by a blank injection (F, L). Total ion chromatograms from RP separations are shown, 1; malonyl-CoA, 2; acetyl-CoA, 3; butyryl-CoA, 4; isovaleryl-CoA, 5; hexanoyl-CoA, 6; octanoyl-CoA, 7; decanoyl-CoA, 8; lauroyl-CoA, 9; myristoyl-CoA, 10; palmitoleoyl-CoA, 11; linoleoyl-CoA, 12; palmitoyl-CoA, 13; oleoyl-CoA, 14; heptadecanoyl-CoA, 15; stearoyl-CoA (C18:0), 16; arachidonoyl-CoA, all at 0.5 μM, 1 pmol on column. Standards were prepared in 1:1 water: MeOH containing 10 mM TEAA.

single gradient with an acidic wash step has positive effects on the elution of acyl-CoAs in the injections that followed, while levels of trapped acyl-CoAs were significantly reduced.

3.3. Harmonizing HILIC and RP methods

Acyl-CoAs ranging from C4-C20 were monitored with the optimized RP method described above (Fig. 2A). Highly polar acyl-CoAs such as C2, 3OH-C4 and malonyl were poorly separated by RP. The same mobile phases were therefore tested on a HILIC column and the same protocol including the 'acidic wash' and 'neutral wash' steps. Buffers at pH 6.5, 7.5 and 8.5 were compared to evaluate the effect of pH on HILIC separation. Although the more hydrophobic compounds (from C4 to C20) were poorly separated, malonyl, 3OH-C4 and C5 were successfully resolved (Fig. 2B). In contrast, *i*C5 could not be separated from *n*C5, even by varying the pH. At higher pH values, acyl-CoAs were less retained on the column and eluted in a higher proportion of ACN, resulting in higher sensitivity.

The separation of *i*C5, 3OH-C4 and malonyl (Fig. 2B) is necessary in order to avoid interference derived from common transitions of these three compounds using the 854 → 347 SRM transition. Specificity of the method for malonyl can be improved if the less abundant but more specific fragment of *m/z* 303 is selected for the SRM transition (see trace of 854 → 303 in Fig. 2B). The fragment of *m/z* 303, formed after a CO_2 loss from the terminal carboxyl group of the malonyl residue and a typical loss for carboxylic acids, is sufficiently specific for malonyl-CoA detection. C5, 3OH-C4 and malonyl are not isomeric compounds, but nevertheless they all provide signal for the same apparent 854 → 347 SRM transition, since the differences between the ion masses of both precursor and product ions of these three compounds are not enough to be separated exclusively on the mass resolving power typical for a triple quadrupole MS/MS (ion formulae and exact ion masses of malonyl, 3OH-C4 and the M + 2 isotopologue of C5 are $C_{24}H_{39}N_7O_{19}P_3S^+$; 854.1229 Da, $C_{25}H_{43}N_7O_{18}P_3S^+$; 854.1593 Da and $C_{24}{}^{13}C_2H_{45}N_7O_{17}P_3S^+$; 854.1867 Da, respectively).

The fact that the same mobile phases used for RP separation were also applicable for HILIC separations facilitated a harmonized setup for fast and comprehensive acyl-CoA profiling in an automated procedure requiring only a total of 32 min.

3.4. Sample preparation strategy

Sample preparation followed the method developed by Minkler et al. for animal tissues [23], modified by the addition of an evaporation/reconstitution step after the SPE, to allow sample concentration and storage. For LC–MS/MS analysis, samples were first reconstituted using water, followed by an appropriate volume of MeOH to a final ratio of 4:1 MeOH:water, which was deemed essential to maintain longer chain (>12 carbons) hydrophobic compounds in solution. When samples were previously reconstituted in as high as 50% aqueous MeOH, the longer chain (C > 12 carbons) acyl-CoAs showed very poor recoveries (i.e. 107% for C4, 92% for C12 but only 33% for C17, 19% for C18:0 and 9% for C20). Although reconstitution in 80% MeOH fits the requirements of the HILIC protocol, it is too strong for the RP separation as early eluting compounds (C2, malonyl) were not adequately retained. Acetyl- and malonyl-CoA were therefore excluded from the RP analysis.

3.5. Acyl-CoA profiling in biological samples

We first tested to what extent the acyl-CoAs included in the targeted method reflect the endogenous species present in mouse liver. C57BL/6 liver tissue was chosen as a representative matrix expected to contain the highest total amount of acyl-CoAs to allow detection of less abundant species. The neutral loss scan mode (NL) of the MS/MS was employed for initial profiling in a non-targeted manner. The 507 Da neutral loss was followed using the precursor mass range of *m/z* 800–1100, a scan rate of 1000 Da/s and 32 V collision energy (CE). The same sample was also analyzed with the targeted SRM method and the resulting chromatograms were compared (Fig. 6).

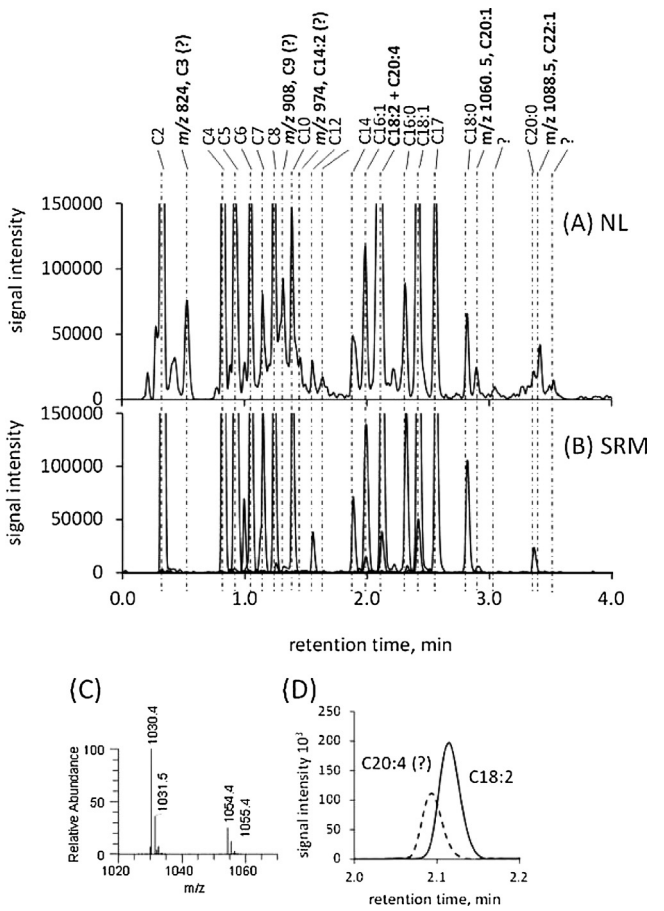

Fig. 6. Acyl-CoA profiles of mouse (C57BL/6) liver. Ion chromatograms were acquired with neutral loss (NL) scan mode (A) and predefined SRM transitions (B) using the same RP separation. Peaks in black are included in the targeted SRM method, identified with reference standards. Peaks in bold are putatively assigned based on precursor ion spectra derived from the NL acquisition. Y-axis is expanded 9× (A) and 15× (B) compared to C2 for better visibility of minor peaks. Example mass spectrum of the two major species found in the precursor ion spectrum at 2.1 min (C) along with the extracted ion chromatograms of *m/z* 1030.4 (C18:2) and *m/z* 1054.4 (putatively assigned as C20:4) (D).

The majority of the compounds that produced prevalent peaks in the NL chromatogram (Fig. 6A) were also present in the targeted SRM method (Fig. 6B), indicating that the SRM method is comprehensive and representative of most acyl-CoAs present in the C57BL/6 liver tissue. Several additional non-targeted species on the NL scan chromatogram (Fig. 6A) could also be putatively identified based on the observed ion masses in the precursor ion spectra derived from the NL acquisition and retention time of closely eluting targeted acyl-CoAs. For example, the prominent peak at 0.58 min with a precursor ion mass of *m/z* 824 most likely corresponds to propionyl-CoA (*n*C3). Similarly, the precursor spectrum of the highly abundant peak at 2.13 min (Fig. 6C) indicates that an abundant compound with *m/z* 1054.4, putatively assigned as C20:4-CoA, co-elutes with C18:2. Extracted ion chromatograms (Fig. 6D) further confirmed this observation. In addition to the primary screening using the TIC of NL, additional compounds were searched for by extracting the (calculated) $[M+H]^+$ ion traces of a number of additional unsaturated acyl-CoAs including decadienoyl-CoA

(C10:2), decenoyl-CoA (C10:1), tetradecadienoyl-CoA (C14:2) and tetradecenoyl-CoA (C14:1), which stem from chain shortening of longer chain unsaturated acyl-CoAs, along with odd chain acyl-CoAs such as nonanoyl-CoA (C9) and undecanoyl-CoA, (C11), which are related to branched chain amino acid metabolism [38]. Chromatographic peaks in the extracted ion chromatograms indicated the presence of additional minor acyl-CoA compounds. Based on the known *m/z* of the $[M+H]^+$ ions of these non-targeted compounds, SRM transitions were defined and incorporated in the SRM method. In addition to two SRM transitions, elution order is considered a very important piece of evidence for the identification, especially when reference standards are not available. In the top panel of Fig. S2, the retention time of C9 and C11 fit perfectly in the elution order of the homologue series of straight chain saturated acyl-CoAs (hydrophobicity increases with chain length of the acyl group in RP chromatography). Similarly, in the mid and bottom pane of Fig. S2, elution order of mono- and di-unsaturated C10:1; C10:2 and C14:1, C14:2, respectively, also fit to the expected elution pattern, i.e., retention time decreases with presence of one or two double bonds.

The developed strategy was also applied to acyl-CoA profiling of HepG2 human liver (Fig. 7D–F) and LHCNM2 human skeletal muscle (Fig. 7G-I) cells, which are more challenging than mouse liver (Fig. 7A–C) due to the limited amount of biological material, especially in the case of LHCNM2 muscle cells. When comparing signal intensities among the three types of biological samples differences in both the profile and abundance already become apparent, which are representative of the studied model. For instance, HepG2 cells are thought to support more lipogenic processes in the absence of exogenous fatty acids [39] as reflected in the higher levels of malonyl-CoA when compared to LHCNM2 muscle cells. Similarly, C16-CoA which is thought to have an important role in fatty acid synthesis and act as a signaling intermediate is about 5x higher in HepG2 compared to LHCNM2 muscle cells. Profiles shown are in agreement with others published in the literature for HepG2 cells [30].

3.6. Quantitative aspects

Recovery studies of acyl-CoAs to address losses during sample preparation (extraction, SPE and evaporation/reconstitution) were initially conducted by addition of 5, 10 or 15 pmol of each standard in the case of cell samples and 50, 100 and 150 pmol of each standard in the case of mouse liver at the extraction step. Considering all three studied matrices and analytes, an average recovery of $64 \pm 10\%$ was obtained. Similar moderate recovery values are reported in the literature for biological samples, independently of the sample preparation method applied [12,16,40]. To address the issue of moderate recovery values, we included surrogate compounds, not present in the matrix, with chemical and physical behavior representative of the native analytes. *N*-Heptadecanoyl-CoA (C17), which could not be detected in either of the original biological sample types and had an average recovery of $58 \pm 6\%$ from all matrices was chosen as an internal standard. Isovaleryl-CoA (*i*C5), with an average recovery of $65 \pm 11\%$, was also tested as an alternative, in order to evaluate whether the chain-length has an influence. As *i*C5 and/or *n*C5 were present in liver tissues at substantial amounts, it was only included in HepG2 and LHCNM2 cell samples, in which it was only present at residual levels compared to the spiked amount (<5% of the level of the spike). Samples from all matrices were prepared again for recovery studies as described above, and 10 or 50 pmol of each surrogate was also added to cell (*i*C5-, C17-CoA) and tissue samples ($(^{13}C_3)$malonyl-, C17-CoA), respectively, prior to sample preparation. For matrix-matched calibrations separate samples were prepared following the same protocol and were spiked with surrogates just before injection at a level identical to the nominal expected concentration in the recovery samples. Un-spiked samples with acyl-CoA standards but with surrogates were also included for "level zero" concentration.

Table 1
Average slope of C17-CoA (ISTD) normalized calibration function of each acyl-CoA in each matrix (n = 3).

	HepG2 cells	C57BL/6 mouse liver tissue	Muscle cells
C4OH-CoA	2.91	1.77	2.21
C4-CoA	3.44	2.29	3.05
C2-CoA	5.10	2.67	3.49
M-CoA	0.20	0.12	0.19
C6-CoA	3.09	1.08	8.09
C7-CoA	3.30	0.76	6.23
C8-CoA	3.75	0.85	5.73
C10:0-CoA	4.86	1.21	6.75
C12:0-CoA	6.79	1.81	8.28
C14:0-CoA	3.32	1.43	5.37
C16:1-CoA	4.10	1.26	5.25
C18:2-CoA	3.91	1.85	5.10
C16:0-CoA	4.68	1.47	5.93
C18:1-CoA	4.50	1.48	4.81
C18:0-CoA	5.27	1.87	7.45
C20:0-CoA	6.15	2.91	12.54

Peak areas normalized to that of the surrogate were used for calculations. Using this approach, and *i*C5 and C17 as surrogate compounds, both with RP and HILIC separations, satisfactory corrections for recoveries between 80–120 % could be achieved in all three studied matrices for the majority of acyl-CoAs. Interestingly, the level of correction was comparable for both surrogates. However, despite satisfactory corrections for the majority of acyl-CoAs, extreme under- or over-corrections were also derived, independently of the surrogate used. For example, in the case of malonyl-CoA, which is generally known to have low recoveries from biological samples [40], only $33 \pm 2\%$ was recovered in our study from mouse liver tissue. Use of C17-CoA as a surrogate was inappropriate for malonyl-CoA correction in this matrix. When $(^{13}C_3)$malonyl-CoA was used, a recovery of $97 \pm 4\%$ was obtained for malonyl-CoA, but the use of this compound overcompensated the recovery of C2 in the HILIC separation which was more accurately corrected by C17.

The use of multiple surrogates, each of them matched in recovery to a subgroup of analytes, is the preferred approach, however not without limitations. As recovery values can be matrix-dependent, if a given surrogate is found to be suitable for a certain matrix it is not necessarily guaranteed to be in another, or *vice versa*. For example, C17 was found to be inappropriate to correct for the low recovery of malonyl-CoA in liver tissue as discussed above, whereas in HepG2 cells the $56 \pm 5\%$ recovery for malonyl-CoA was corrected to $93 \pm 5\%$ and $83 \pm 6\%$ with C17 and *i*C5 respectively. Furthermore, apart from $(^{13}C_3)$ isotopes, it is difficult to find surrogates that represent the chemical behavior of a native analyte closely enough and at the same time are not endogenously present in the sample.

As an alternative for using individual isotope-enriched acyl-CoA standards, most of which are not commercially available, a standard type addition protocol is suggested such as the one described for recovery and calibration studies here. Samples were spiked with standard mixtures at multiple levels and with constant levels of surrogates as described above, prior to sample preparation. Peak areas normalized to that of the respective surrogate were used to set up calibration curves. Concentrations of different species were derived based on the peak area of the analyte normalized to that of the surrogate, divided by the slope of the calibration function of the corresponding analyte in the specific matrix (Table 1). Recoveries ranging between 90–111, 90–109 and 98–104% were obtained for

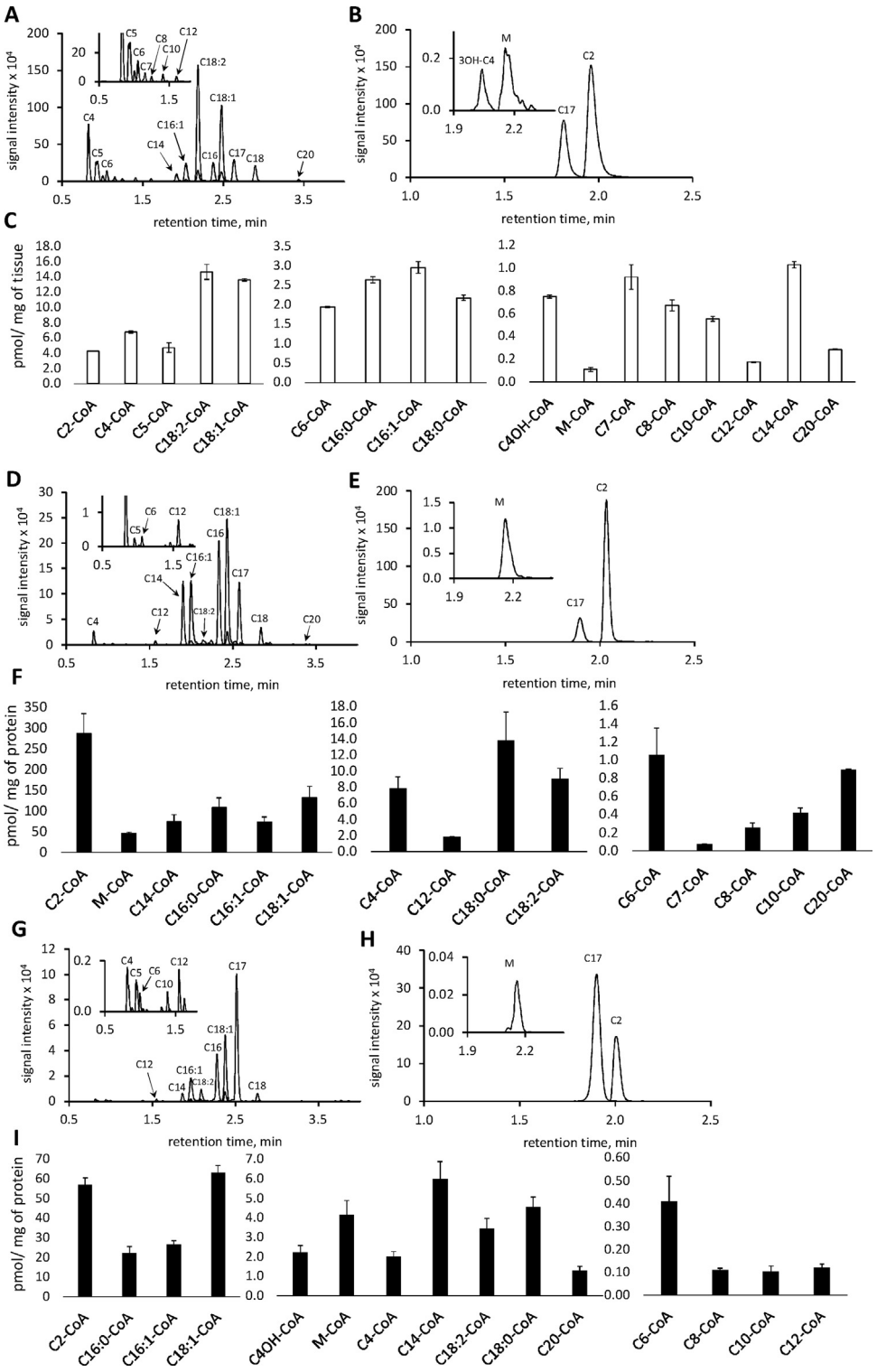

Fig. 7. Typical acyl-CoA profiles and levels in C57BL/6 mouse liver tissue (A–C) hepatic (HepG2) ((D–F)) and muscle (LHCNM2) ((G–I)) cells.Overlaid SRM chromatograms acquired with RP chromatography are shown in panels A, D, G and with HILIC separation in panels B, E, H. Internal standard (C17) is present at 0.2 μM in cell samples (C–F) and 0.5 μM in mouse liver samples (A, B). Error bars represent SD of three independent samples in each group (n = 3).

all analytes in the C57BL/6 liver tissue, HepG2 cells and muscle cells respectively.

In HepG2 cells (from one 6-well of ∼ 9.5 cm^2 surface area, containing ∼ 200 μg protein from ∼ 1.5×10^6 cells), individual acyl-CoAs were in the range of 0.3–286 pmol/mg protein (2-2300 fmol acyl-CoAs on column) (Fig. 7F) while a single 6-well of LHCNM2 cells typically contained 0.2–65 pmol/mg protein (1–260 fmol acyl-CoAs on column) in ∼ 4×10^5 cells (∼ 100 μg protein) (Fig. 7I), ∼ 5-fold lower in comparison to HepG2 cells. Detected acyl-CoA species in liver tissue were in the range of 0.1–4.8 pmol/mg (40–2000 fmol acyl-CoAs on column) when starting from ∼ 20 mg sample (Fig. 7C). Despite the low amounts of acyl-CoAs present, samples were stable for >24 h in the auto-sampler at 10 °C, in contradiction to other authors, who reported increasing hydrolysis of

Table 2
Method detection limits (MDL) of each acyl-CoA.[a]

	Acyl-CoA	MDL, nM	fmol on column (2 uL inj)
HILIC	C4OH-CoA	0.7	1.4
	C2-CoA	1.5	3.1
	M-CoA	1.2	2.4
	C4-CoA	1.9	3.8
C18	C6-CoA	1.6	3.3
	C7-CoA	0.7	1.4
	C8-CoA	1.5	3.0
	C10:0-CoA	1.6	3.2
	C12:0-CoA	1.1	2.2
	C14:0-CoA	1.4	2.9
	C16:1-CoA	1.6	3.1
	C18:2-CoA	2.4	4.9
	C16:0-CoA	0.5	1.1
	C18:1-CoA	2.3	4.6
	C18:0-CoA	1.9	3.9
	C20:0-CoA	1.2	2.3

[a] Method Detection Limits (MDL) were calculated using the protocol suggested by the US EPA [25].

the acyl-CoAs with the acyl chain length [30] as a possible explanation. We believe the instability issues reported by others are a function of the analytes precipitating in solution due to insufficient ionic and organic strength of the applied solvent for sample preparation and chromatography issues as discussed here.

In cases where the amount of available sample is highly limited (e.g., LHCNM2 cells), the detection power of the analytical system is crucial. The extensively used method to determine detection limits (LOD) based on the estimation of signal-to-noise ratios (S/N) in blank samples was considered inappropriate in our study due to the high specificity of the SRM (MRM) mode that resulted in zero system background noise. This leads to infinite S/N that offsets realistic estimation of LODs. An alternative approach was applied and LODs were estimated by analyzing a series of dilutions of standard mixtures to find the lowest concentration at which the analytes could be detected. The 0.5 nM level was found to be the lowest level where all acyl-CoA species produced identifiable chromatographic peaks. However, note that at that low level, which can be considered as the realistic LOD of the method, the repeatability of measurement substantially deteriorated. If the Method Detection Limits (MDL) were calculated using the protocol suggested by the US EPA [41], where repeatability is accounted for, MDL values ($\alpha = 0.01$, $t_\alpha = 2.76$) between 0.5–2.4 nM were obtained that correspond to 1–4.9 fmol analyte on column (Table 2) based on the applied 2 μL injection volume. Even though in most reports LODs are calculated based on the S/N = 3 approach, which presumably results in better than realistic LODs, the LODs achieved with this method are substantially superior to the ones reported in literature based on 3x S/N. For instance, Kasuya et al. [12] reported detection limits of palmitoyl-CoA, arachidonoyl-CoA and octanoyl-CoA, of 60, 92 and 51 fmol, respectively, Yang et al. [30] reported LODs of 70–140 fmol for C10:0 to C20:0 acyl-CoAs, whereas Li et al. [19] reported 40 fmol for malonyl-CoA and C8 and 142 fmol for C16.

4. Conclusions

In the work presented here, we aimed to describe optimal chromatographic conditions for reproducible analysis of acyl-CoAs from various matrices and discuss how their low abundance and nature may challenge the robustness of previous approaches. The UHPLC–ESI-MS/MS analytical system developed was equally suitable for high sensitivity analysis of short-, medium, and long chain acyl-CoAs spanning from acetyl- (C2:0) to arachidonoyl-CoA (C20:0) in biological samples. When fold changes of acyl-CoAs are of primary study interest, we propose that the use of C17 is practical and necessary both to enable corrections for occasional sample losses during sample preparation and for routine fluctuations of the MS signal, for the majority of acyl-CoAs in cellular samples, but not for malonyl-CoA. The developed harmonized dual chromatographic method enables both RP and HILIC analyses from the same sample that remarkably improves the throughput of the assay. The enhanced sensitivity achieved enables analysis of small biological samples which is of particular importance in the case of cellular experiments and clinical biopsies, and can help unravel the role of these important intermediate signaling molecules in cellular energy balance.

Acknowledgements

This research was supported by a European Research Council Advanced Grant (POLYTRUE? 322467). LHCNM2 immortalized human skeletal muscle cells were a gift from Dr. Vincent Mouly, UMR S 787 (INSERM & UPMC), Institut de Myologie, Faculté de Médecine Pierre et Marie Curie, Paris, France. The authors wish to thank Dr. Kornel Nagy (Nestlé Research Center, Lausanne, Switzerland) for valuable input at the early stages of this work and Professor Mike Clifford (Emeritus Professor, University of Surrey, UK) for fruitful discussions during the revision process.

Appendix A. Supplementary data

Supplementary material related to this article can be found, in the online version, at doi:https://doi.org/10.1016/j.chroma.2017.12.052

References

[1] L.O. Li, E.L. Klett, R.A. Coleman, Acyl-CoA synthesis, lipid metabolism and lipotoxicity, Biochim. Biophys. Acta (BBA) – Mol. Cell Biol. Lipids 1801 (2010) 246–251.
[2] M.T. Nakamura, B.E. Yudell, J.J. Loor, Regulation of energy metabolism by long-chain fatty acids, Prog. Lipid Res. 53 (2014) 124–144.
[3] T. Mauriala, K.H. Herzig, M. Heinonen, J. Idziak, S. Auriola, Determination of long-chain fatty acid acyl-coenzyme A compounds using liquid chromatography–electrospray ionization tandem mass spectrometry, J. Chromatogr. B 808 (2004) 263–268.
[4] M.A.D.N. Perera, S.-Y. Choi, E.S. Wurtele, B.J. Nikolau, Quantitative analysis of short-chain acyl-coenzyme as in plant tissues by LC–MS–MS electrospray ionization method, J. Chromatogr. B 877 (2009) 482–488.
[5] J.J. Dalluge, S. Gort, R. Hobson, O. Selifonova, F. Amore, R. Gokarn, Separation and identification of organic acid-coenzyme A thioesters using liquid chromatography/electrospray ionization-mass spectrometry, Anal. Bioanal. Chem. 374 (2002) 835–840.
[6] L. Gao, W. Chiou, H. Tang, X. Cheng, H.S. Camp, D.J. Burns, Simultaneous quantification of malonyl-CoA and several other short-chain acyl-CoAs in animal tissues by ion-pairing reversed-phase HPLC/MS, J. Chromatogr. B 853 (2007) 303–313.
[7] A.U. Blachnio-Zabielska, C. Koutsari, M.D. Jensen, Measuring long-chain acyl-coenzyme A concentrations and enrichment using liquid chromatography/tandem mass spectrometry with selected reaction monitoring, Rapid Commun. Mass Spectrom. 25 (2011) 2223–2230.
[8] N.W. Snyder, S.S. Basu, Z. Zhou, A.J. Worth, I.A. Blair, Stable isotope dilution liquid chromatography/mass spectrometry analysis of cellular and tissue medium- and long-chain acyl-coenzyme A thioesters, Rapid Commun. Mass Spectrom. 28 (2014) 1840–1848.
[9] S.S. Basu, I.A. Blair, SILEC: a protocol for generating and using isotopically labeled coenzyme A mass spectrometry standards, Nat. Protocols 7 (2012) 1–12.
[10] C.A. Haynes, J.C. Allegood, K. Sims, E.W. Wang, M.C. Sullards, A.H. Merrill Jr., Quantitation of fatty acyl-coenzyme As in mammalian cells by liquid chromatography-electrospray ionization tandem mass spectrometry, J. Lipid Res. 49 (2008) 1113–1125.
[11] B. Kalderon, V. Sheena, S. Shachrur, R. Hertz, J. Bar-Tana, Modulation by nutrients and drugs of liver acyl-CoAs analyzed by mass spectrometry, J. Lipid Res. 43 (2002) 1125–1132.
[12] F. Kasuya, T. Masuyama, T. Yamashita, K. Nakamoto, S. Tokuyama, H. Kawakami, Determination of acyl-CoA esters and acyl-Co A synthetase activity in mouse brain areas by liquid chromatography-electrospray ionization-tandem mass spectrometry, J. Chromatogr. B: Anal. Technol. Biomed. Life Sci. 929 (2013) 45–50.

[13] A.A. Palladino, J. Chen, S. Kallish, C.A. Stanley, M.J. Bennett, Measurement of tissue acyl-CoAs using flow-injection tandem mass spectrometry: acyl-CoA profiles in short-chain fatty acid oxidation defects, Mol. Genet. Metab. 107 (2012) 679–683.
[14] R.W. Purves, S.J. Ambrose, S.M. Clark, J.M. Stout, J.E. Page, Separation of isomeric short-chain acyl-CoAs in plant matrices using ultra-performance liquid chromatography coupled with tandem mass spectrometry, J. Chromatogr. B 980 (2015) 1–7.
[15] C.A. Haynes, Analysis of mammalian fatty acyl-coenzyme A species by mass spectrometry and tandem mass spectrometry, Biochim. Biophys. Acta – Mol. Cell Biol. Lipids 1811 (2011) 663–668.
[16] C. Magnes, F.M. Sinner, W. Regittnig, T.R. Pieber, LC/MS/MS method for quantitative determination of long-chain fatty acyl-CoAs, Anal. Chem. 77 (2005) 2889–2894.
[17] C. Magnes, M. Suppan, T.R. Pieber, T. Moustafa, M. Trauner, G. Haemmerle, F.M. Sinner, Validated comprehensive analytical method for quantification of coenzyme A activated compounds in biological tissues by online solid-phase extraction LC/MS/MS, Anal. Chem. 80 (2008) 5736–5742.
[18] M. Zimmermann, V. Thormann, U. Sauer, N. Zamboni, Nontargeted profiling of coenzyme A thioesters in biological samples by tandem mass spectrometry, Anal. Chem. 85 (2013) 8284–8290.
[19] Q. Li, S. Zhang, J.M. Berthiaume, B. Simons, G.F. Zhang, Novel approach in LC-MS/MS using MRM to generate a full profile of acyl-CoAs: discovery of acyl-dephospho-CoAs, J. Lipid Res. 55 (2014) 592–602.
[20] A. Wakamatsu, K. Morimoto, M. Shimizu, S. Kudoh, A severe peak tailing of phosphate compounds caused by interaction with stainless steel used for liquid chromatography and electrospray mass spectrometry, J. Sep. Sci. 28 (2005) 1823–1830.
[21] A.V. Qualley, B.R. Cooper, N. Dudareva, Profiling hydroxycinnamoyl-coenzyme A thioesters: unlocking the back door of phenylpropanoid metabolism, Anal. Biochem. 420 (2012) 182–184.
[22] E.R. Stadtman, Preparation and assay of acyl coenzyme A and other thiol esters; use of hydroxylamine, Methods Enzymol. (1957) 931–941.
[23] P.E. Minkler, J. Kerner, S.T. Ingalls, C.L. Hoppel, Novel isolation procedure for short-, medium-, and long-chain acyl-coenzyme A esters from tissue, Anal. Biochem. 376 (2008) 275–276.
[24] A.B. Hummon, S.R. Lim, M.J. Difilippantonio, T. Ried, Isolation and solubilization of proteins after TRIZOL® extraction of RNA and DNA from patient material following prolonged storage, BioTechniques 42 (2007) 467–472.
[25] N.A. Corfu, H. Sigel, Acid-base properties of nucleosides and nucleotides as a function of concentration, Eur. J. Biochem. 199 (1991) 659–669.
[26] W.L. Masterton, C.N. Hurley, Chemistry: Principles and Reactions, 5th (2003) ed., Thomson-Brooks/Cole, London, 1927.
[27] M. Mateos-Vivas, E. Rodríguez-Gonzalo, D. García-Gómez, R. Carabias-Martínez, Hydrophilic interaction chromatography coupled to tandem mass spectrometry in the presence of hydrophilic ion-pairing reagents for the separation of nucleosides and nucleotide mono-, di- and triphosphates, J. Chromatogr. A 1414 (2015) 129–137.
[28] J. Kim, D.G. Camp Ii, R.D. Smith, Improved detection of multi-phosphorylated peptides in the presence of phosphoric acid in liquid chromatography/mass spectrometry, J. Mass Spectrom. 39 (2004) 208–215.
[29] X. Liu, S. Sadhukhan, S. Sun, G.R. Wagner, M.D. Hirschey, L. Qi, H. Lin, J.W. Locasale, High-resolution metabolomics with acyl-CoA profiling reveals widespread remodeling in response to diet, Mol. Cell. Proteomics 14 (2015) 1489–1500.
[30] X.K. Yang, Y.J. Ma, N. Li, H.J. Cai, M.G. Bartlett, Development of a method for the determination of Acyl-CoA compounds by liquid chromatography mass spectrometry to probe the metabolism of fatty acids, Anal. Chem. 89 (2017) 813–821.
[31] R. Tuytten, F. Lemière, E. Witters, W.V. Dongen, H. Slegers, R.P. Newton, H.V. Onckelen, E.L. Esmans, Stainless steel electrospray probe: a dead end for phosphorylated organic compounds? J. Chromatogr. A 1104 (2006) 209–221.
[32] H. Sakamaki, T. Uchida, L.W. Lim, T. Takeuchi, Evaluation of column hardware on liquid chromatography-mass spectrometry of phosphorylated compounds, J. Chromatogr. A 1381 (2015) 125–131.
[33] P.R. Haddad, R.C.L. Foley, Contamination of aqueous eluents due to corrosion of stainless-steel chromatographic components, J. Chromatogr. A 407 (1987) 133–140.
[34] P.P. Constantinides, J.M. Steim, Solubility of palmitoyl-coenzyme A in acyltransferase assay buffers containing magnesium ions, Arch. Biochem. Biophys. 250 (1986) 267–270.
[35] J. Zhang, Q. Wang, B. Kleintop, T. Raglione, Suppression of peak tailing of phosphate prodrugs in reversed-phase liquid chromatography, J. Pharm. Biomed. Anal. 98 (2014) 247–252.
[36] R. Harmancey, C.R. Wilson, N.R. Wright, H. Taegtmeyer, Western diet changes cardiac acyl-CoA composition in obese rats: a potential role for hepatic lipogenesis, J. Lipid Res. 51 (2010) 1380–1393.
[37] Y. Asakawa, N. Tokida, C. Ozawa, M. Ishiba, O. Tagaya, N. Asakawa, Suppression effects of carbonate on the interaction between stainless steel and phosphate groups of phosphate compounds in high-performance liquid chromatography and electrospray ionization mass spectrometry, J. Chromatogr. A 1198–1199 (2008) 80–86.
[38] S.B. Crown, N. Marze, M.R. Antoniewicz, Catabolism of branched chain amino acids contributes significantly to synthesis of odd-chain and even-chain fatty acids in 3T3-L1 adipocytes, PLoS One 10 (2015).
[39] V.W. Daniëls, K. Smans, I. Royaux, M. Chypre, J.V. Swinnen, N. Zaidi, Cancer cells differentially activate and thrive on de novo lipid synthesis pathways in a low-lipid environment, PLoS One 9 (2014).
[40] P.E. Minkler, J. Kerner, T. Kasumov, W. Parland, C.L. Hoppel, Quantification of malonyl-coenzyme A in tissue specimens by high-performance liquid chromatography/mass spectrometry, Anal. Biochem. 352 (2006) 24–32.
[41] J.M. Ntambi, M. Miyazaki, Regulation of stearoyl-CoA desaturases and role in metabolism, Prog. Lipid Res. 43 (2004) 91–104.